Nano Biomed Eng
2019, 11(1): 58-66. doi: 10.5101/nbe.v11i1.p58-66.

Research Article

Biofabrication of Gold Nanoparticles Using *Cressa cretica* Leaf Extract and Evaluation of Catalytic and Antibacterial Efficacy

Subramanian Balasubramanian[1,2], Soosaimichael Mary Jelastin Kala[1], Thomas Lurthu Pushparaj[3], Paulraj Vijaya Kumar[1]

[1]Research Centre, Department Of Chemistry, St. Xaviers College, Palayamkottai, Tirunelveli-627002, India.
[2]Department of Chemistry, A.R. College of Engineering & Technology, Kadayam, Tirunelveli-627423, India.
[3]Department of Chemistry, Einstein College of Engineering, Tirunelveli - 627012, India.

Corresponding author. E-mail: bensosurya@yahoo.com

Received: Jul. 24, 2018; **Accepted:** Jan. 9, 2019; **Published:** Mar. 7, 2019.

Citation: Subramanian Balasubramanian, Soosaimichael Mary Jelastin Kala, Thomas Lurthu Pushparaj, and PaulrajVijaya Kumar, Biofabrication of Gold Nanoparticles Using *Cressa cretica* Leaf Extract and Evaluation of Catalytic and Antibacterial Efficacy. *Nano Biomed. Eng.*, 2019, 11(1): 58-66.
DOI: 10.5101/nbe.v11i1.p58-66.

Abstract

Biofabrication of nanoparticles using plant sources is considered the most vital method for nanoparticle syntheses, as the use of plant materials not only makes the process eco-friendly but also its abundance makes it less expensive. In this study, we aimed to develop a rapid and simple procedure for the synthesis of gold nanoparticles using aqueous *Cressa cretica* leaf extract as a reducing agent as well as a capping agent. The characteristics of biofabricated gold nanoparticles were examined using ultraviolet-visible absorption spectroscopy (UV-Vis), Fourier-transform infrared spectroscopy (FTIR), scanning electron microscope (SEM), X-ray powder diffraction (XRD) and energy dispersive X-ray spectroscopy (EDX). As the results, the biofabricated gold nanoparticles were of hexagonal, pentagonal, spherical and rod shapes with 15-22 nm in size. FTIR studies disclosed that hydroxyl, amide and amine groups of *Cressa cretica* leaf broth were liable for the formation and stabilization of the gold nanoparticles. The antibacterial activity of the gold nanoparticles against human pathogens showed significant zones of inhibition. It confirmed that the biofabricated gold nanoparticles have great promise as an antibacterial agent. The biofabricated gold nanoparticles were used as catalysts in the reduction of 4-nitrophenol using sodium borohydride. The catalytic activity studies exhibited that the biofabricated gold nanoparticles had prominent catalytic activity. Furthermore, this green biofabric approach is a fast and easy alternative to chemical synthesis.

Keywords: Biosynthesis; Gold nanoparticles; *Cressa cretica*; Antibacterial efficacy; Catalysis; 4-Nitrophenol

Introduction

Nanotechnology is an interdisciplinary area of research interlarding bionanotechnology and material science. Significant advances in nanotechnology and biotechnology are made to gain the benefit of life sciences, healthcare and industrial biotechnology [1-3]. There is prominent interest in the synthesis of noble metal nanoparticles for their applications such as electronics, catalysis, optics and biomedical [4, 5]. The method of preparation of nanoparticles using chemical and physical techniques is more expensive,

hazardous to the environment and needed high energy consumption. Biosynthesis of nanoparticles is a simple technique, but its applications are prominent in human welfare. Biological methods using microorganisms, enzymes, fungi and plant parts are more eco-friendly alternatives than chemical and physical methods [6-9]. In biosynthesis, use of plant parts is favourable than other biological approaches by eliminating the method of maintaining the time-consuming aseptic microbial culture. Plant meditated nanoparticles are more stable, low cost and eco-friendly [10-13].

Recently, plant extracts have been studied to exhibit high efficacy in metal nanoparticles syntheses such as *Jasminum auriculatum* [14], *Anacardium occidentale* [15], *Cressa cretica* [16], *Alpinia nigra* [17], etc. Biomolecules (e.g. terpenoids, flavonoids, alkaloids and phenolic compounds) present in plant extract can be employed to reduce metal ions to form metal nanoparticles and to stabilize metal nanoparticles in a single step biofabrication process [18-20].

Metal nanoparticles can act as an antimicrobial agent due to their ability to interact with microorganisms. Gold nanoparticles are extensively employed in organisms due to bioconjugation abilities, its biocompatible nature, strong scattering and absorbing properties, as target drug delivery in various therapeutics and cancer treatment. Gold nanoparticles (Au NPs) have been reported to possess great antimicrobial activities and catalytic activity in 4-nitrophenol reduction [21-25]. A number of studies have illustrated the biosynthesis of Au NPs using the subsequent plant extract as reducing agents and catalysts in the 4-nitrophenol reduction reaction: *Aerva lanata* [26], *Phoenix dactylifera* [27] and *Garcinia combogia* [28]. The reaction product, 4-aminophenol, is a vital intermediate for antipyretics and analgesics.

Uppu Marikkozhundu is widely distributed throughout India. The scientific name of the Uppu Marikkozhundu medicinal plant is *Cressa cretica*. The medicinal plant is a small dwarf shrub. *Cressa cretica* plant is generally known in Sanskrit as Sanjeevani as it prolongs the human life and obstructs the onset of old age. In Ayurveda, the *Cressa cretica* plant parts play a major role in curing different diseases such as constipation, leprosy, asthma, and urinary discharges, diabetes and general debility. The *Cressa cretica* plant is utilized as tonic, anthelmintic, stomachic and enriches the blood, aphrodisiac purposes [29, 30]. In the present study, to the best of our knowledge, biofabrication of gold nanoparticles has been reported for the first time using *Cressa cretica* leaf extract both, as a reducing and capping agent. We have examined the optical, morphological, catalytic and antibacterial characteristics of biofabricated Au NPs using *Cressa cretica* leaf extract.

Experimental Methods

Preparation of *Cressa cretica* leaf extract

Cressa cretica (*C. cretica*) plants were gathered from Tuticorin District, Tamilnadu, India. The *C. cretica* plant leaves were washed thoroughly first with tap water to remove the adhering particles, then with distilled water. The purified *Cressa cretica* leaves were desiccated in shadow for 9 days. The desiccated *Cressa cretica* leaves were crushed using mortar and pestle. The powdered C. cretica leaf was weighed (10 g) and mixed with 100 mL of distilled water in a 250 mL beaker. The mixture was boiled at 80 °C for 20 min and filtered through Whatman No. 1 filter paper to get the *C. cretica* leaf broth. The filtrate was collected and stored at 5 °C.

Synthesis of gold nanoparticles

Gold (III) chloride trihydrate solution (1 mM) was prepared using 100 mL of distilled water. 10 mL of *Cressa cretica* leaf extract was mixed with 90 mL of 1 mM gold (III) Chloride trihydrate ($HAuCl_4 \cdot 3H_2O$) solution in a 250 mL beaker. The resultant mixture was permitted to incubate at room temperature. The resulting mixture turned from yellow to ruby red in colour within 2 h due to gold nanoparticles formation [27].

Characterization

The pH of gold chloride solution and *Cressa cretica* leaf extract was measured using a digital pH meter (Roy instruments RI 501). The gold (III) chloride solution (1 mM) showed pH 6.23. The *Cressa cretica* leaf extract's pH was 9.34. The pH of the reaction mixture was observed using the digital pH meter during biofabrication of gold nanoparticles. The ultraviolet-visible absorption spectra of the gold nanoparticles were recorded using an ultraviolet-visible spectrophotometer (LABMAN, LMSP-UV1900S) at room temperature. The scanning range for the Au NPs was 300-800 nm with a resolution of 1 nm. Fourier-transform infrared (FTIR) spectra of the *Cressa cretica* leaf extract and the Au NPs were recorded using FTIR spectrophotometer (IR Tracer-100 Shimadzu) in the range from 4,000 to 400 cm^{-1}. The biofabricated Au NPs were purified by repeated centrifugation at a speed

of 10,000 rpm for 25 min to remove excess starting materials. The Au NPs pellets were dried using a hot air oven at 60 °C. The dried biofabricated Au NPs were probed using Bruker X-Ray Diffractometer (D8 Advance ECO XRCD Systems with SSD160 1 D Detector). Scanning electron microscopy analysis was carried out to determine the structure and size of the Au NPs using a scanning electron microscope (SEM) Carl Zeiss EVO18. The chemical purity and elemental composition of the Au NPs were analysed using an energy dispersive X-ray spectrometer (OXFORD XMX N).

Antibacterial activity of Au NPs

The antimicrobial assays were carried out on human pathogenic bacteria such as *Streptococcus pyogenes*, *Staphylococcus aureus*, *E. coli* and *Klebsiella pneumoniae* by disc diffusion method using antibiotic chloramphenicol as standard [31, 32]. Muller Hinton agar medium was used to cultivate bacteria. The different concentrations of 10 µL, 20 µL and 30 µL (100 µg/mL) of Au NPs suspension were prepared by reconstituting with methanol. The four clinical micro-organisms are swapped over the agar medium using sterilized tongs, and the biofabricated Au NPs containing discs were kept over the medium using sterilized tongs and incubated at 37 °C for 24 h. The zone of inhibition of the gold nanoparticles was measured in mm and taken as their antibacterial efficacy against the test pathogen.

Catalytic activity of Au NPs

The catalytic efficacy of biofabricated gold nanoparticles was scrutinized by the reduction of 4-nitrophenol to 4-aminophenol using sodium borohydride solution [33]. This reduction reaction was observed using UV-Vis spectroscopy in the range of 250-600 nm. Typically, 0.5 mL of 10 mM sodium borohydride was mixed with 0.5 mL of distilled water and 2 mL of 1.5 mM 4-nitrophenol in a quartz cuvette. Then 0.5 mL (1mg/mL) of the gold nanoparticles were mixed with the reaction mixture in the quartz cuvette. The resultant mixture was monitored using ultraviolet-visible spectroscopy (UV-Vis) in the range of 250-600 nm at periodic time intervals.

Results and Discussion

Variation in pH during synthesis of gold nanoparticles (Au NPs)

The pH of the reaction mixture reduced from 7.64 to 6.14 in presence of *Cressa cretica* leaf extract showing a reduction of 1 mM $HAuCl_4 \cdot 3H_2O$ solution during formation of gold nanoparticles. During the biofabrication of gold nanoparticles, the pH of the reaction mixture was diminished. Similar results were previously reported using *Tecomella undulata* leaf extract for green synthesised silver nanoparticles [34].

Visual investigation and ultraviolet-visible spectroscopy (UV-Vis)

The reduction of Au^{3+} into Au NPs during exposure to *Cressa cretica* leaf extract was visually evident from the colour change of reaction mixture from light yellow to ruby red, as a result of the surface plasmon resonance phenomenon (Fig. 1). The colour change was observed within 2 h, indicating the formation of Au NPs. UV-Vis was used to determine the formation of gold nanoparticles. In the UV-Vis spectrum (Fig. 2), a sharp intense and broad peak at 539 nm was obtained, which corresponds to the typical surface plasmon resonance of gold nanoparticles [35]. The widening of peak suggested that the particles were polydisperse. Similar results were reported using *Anacardium occidentale* leaf extract for gold nanoparticles [15].

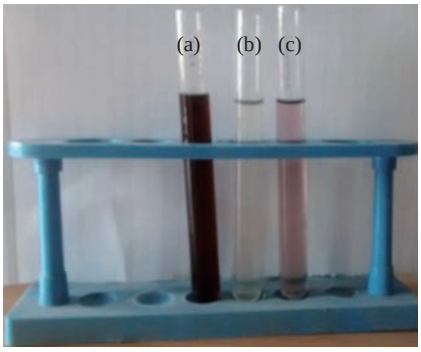

Fig. 1 Photograph of biofabrication of gold nanoparticles: **(a)** Aqueous *C. cretica* leaf extract; **(b)** $HAuCl_4 \cdot 3H_2O$ solution; and **(c)** Colloidal gold nanoparticles solution using *C. cretica* leaf extract.

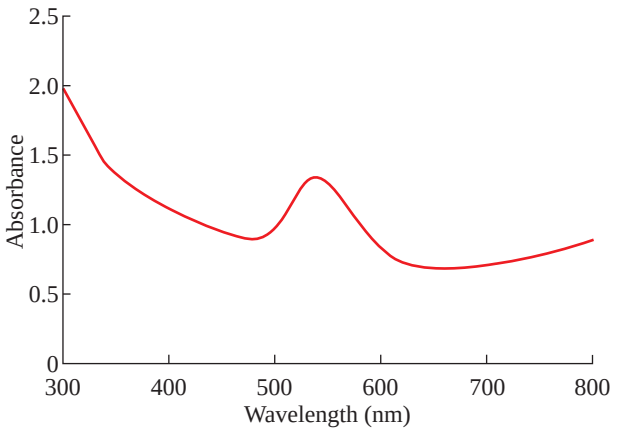

Fig. 2 Ultraviolet-visible absorption spectra of gold nanoparticles using *C. cretica* leaf extract.

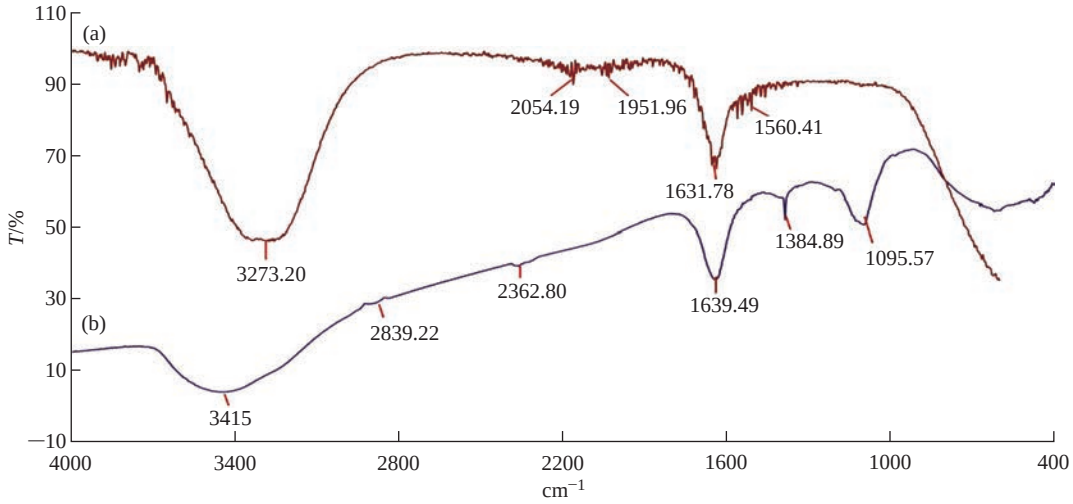

Fig. 3 Fourier-transform infrared spectra of **(a)** *C. cretica* leaf extract and **(b)** Au NPs using *C. cretica* leaf extract.

Fourier-transform infrared spectroscopy (FTIR) analysis

The FTIR spectra of the *Cressa cretica* leaf extract and biofabricated Au NPs are shown in Fig. 3. The FTIR spectrum of the *Cressa cretica* leaf extract showed peaks at 3273.20 cm^{-1} (O-H stretch of alcohol/ phenols/amine), 2054.19 cm^{-1} (N-H stretch of amines), 1951.96 cm^{-1} (C–C stretch of aromatic alkanes), 1631.78 cm^{-1} (C=O stretch of amides) and 1560.41 cm^{-1} (N-H stretch of aliphatic amines), whereas that of the Au NPs showed peaks at 3415 cm^{-1} (O-H stretch of alcohol/phenols/amine), 2839.22 cm^{-1} (H-C-(O) stretch of aldehyde/ aromatic alkanes), 2362.80 cm^{-1} (N-H stretch of amines), 1639.49 cm^{-1} (C=O stretch of amides), 1384.89 cm^{-1} (NO_2 stretch of nitro compounds) and 1095.57 cm^{-1}(C-O stretch of ester/ lactones) [36]. The characteristic hydroxyl group was observed in the leaf extract at 3273.20 cm^{-1}. This peak was shifted to 3415 cm^{-1} in the Au NPs. A peak associated with the N–H stretching of amines appeared at 2054.19 cm^{-1} in the spectrum of the *Cressa cretica* leaf extract, and this peak was shifted to 2362.80 cm^{-1} after the synthesis of the Au NPs. The characteristic C=O group of amide was observed in the leaf extract at 1631.78 cm^{-1}. This peak was shifted to 1639.49 cm^{-1} in the Au NPs. As the results of band shift in the amine, amide and hydroxyl groups, the amine, amide and hydroxyl groups of *Cressa cretica* leaf extract are involved in the formation and stabilization of the gold nanoparticles. Furthermore, three peaks were found at 2839.22 cm^{-1}, 1384.89 cm^{-1} and 1095.57 cm^{-1} in the Au NPs, corresponding to aldehyde, nitro groups and ketone groups respectively. The appearance of these three peaks in Au NPs implied that the amide/ amine groups were converted into nitro groups, and the alcoholic group was converted into aldehyde/ ketone to reduce Au^{3+} to Au^0. The observed peaks were more characteristic of flavonoids, steroids, phenolic compounds, and amino acids which are abundant in *Cressa cretica* leave extracts [29]. FTIR results suggest that the flavonoids, steroids, phenolic compounds, and amino acids present in the *Cressa cretica* leaf extract are mostly involved in the reduction of Au^{3+}ions and/or are complexed (or adsorbed) on the surface of biosynthesized Au NPs.

X-ray powder diffraction (XRD) analysis

The XRD pattern of the gold nanoparticles is represented in Fig. 4. The XRD pattern displayed intense peaks in the whole spectrum of 2θ values, ranging from 30° to 90°. The peaks at 2θ values of 37.73°, 44.94°, 64.42° and 77.31° correspond to (111), (200), (220) and (311) for fcc gold nanoparticles. A comparison of our sample XRD pattern with the standard sample (JCPDS file no: 04-0784) confirmed that the biofabricated gold nanoparticles using *C. cretica* leaf extract had been formed in the form of

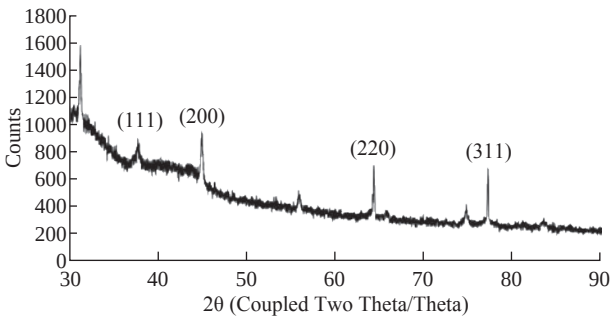

Fig. 4 X-ray powder diffraction patterns of gold nanoparticles using *C. cretica* leaf extract.

crystalline. Thus, the XRD pattern exhibited that the gold nanoparticles using *Cressa cretica* leaf extract were crystalline in nature. The average crystallite size of the gold nanoparticles was found using Debye–Scherrer formula:

$$D=K\lambda/\beta\cos\theta,$$

where D is the average crystallite size (nm), K is the Scherrer constant, β is the full width at half maximum, θ is half of Bragg angle, and λ is the wavelength of X-ray used. The average crystallite size of the gold nanoparticles using *C. cretica* leaf extract was around 15-22 nm. These results are comparable to those in a previously studied by Wani et al. [37], using *Nepenthes khasiana* leaf extract [38] and *Dillenia indica* fruit extract [39] for gold nanoparticles.

Scanning electron microscope (SEM) and energy dispersive X-ray spectroscopy (EDX) analyses

The surface morphology and the topography of biofabricated gold nanoparticles were examined using SEM analysis. SEM micrographs (Fig. 5) showed that the gold nanoparticles were relatively hexagonal, pentagonal, spherical and rod in shape, and polydispersed without aggregation in solution. The presence of surplus amounts of reducing moieties and the interactions between stabilizing molecules bound to the surface of nanoparticles and secondary reduction process on the surface of the preformed nuclei, resulting aggregation of two or more nanoparticles together. This can be cited as a reason for the formation of large-size particles [40]. The size of the Au NPs was found to be in the range of 15-22 nm. The similar the range of gold nanoparticles formed using *Artemisia capillaris* extract [41], *Diospyros ferrea* plant extract [42] and *Dendropanax morbifera* leaf extract [43].

The elemental composition of the biofabricated Au NPs was evaluated using EDX analysis. In the EDX spectrum (Fig. 6), the signals were observed at approximately 2.2, 8.42, 9.68, 11.5 and 13.42 keV corresponded to the gold element. It revealed the existence of gold nanoparticles. The other signals for Na, S, Cl, O, Mg and K were observed, which arose from enzymes or proteins present within *Cressa cretica* leaf extract. The results were analogous to Wang et al's results [43].

Antimicrobial activity of gold nanoparticles

The antibacterial efficacy of the biofabricated Au NPs was measured against bacteria such as gram-positive bacteria (*Streptococcus pyogenes, Staphylococcus aureus*) and gram-negative bacteria (*Escherichia coli, Klebsiella pneumoniae*) using well diffusion method [44]. The Au NPs inhibited the growth of bacteria which formed inhibition zones as shown in Fig. 7. The inhibition zones of Au NPs are illustrated using Table1. The high inhibition zone in the 30 µL (100 µg/mL) concentration of the Au NPs was 12 mm for *Streptococcus pyogenes*, 8 mm for *Staphylococcus aureus*, 10 mm for *Escherichia coli* and 7 mm for *Klebsiella pneumoniae*, respectively. The highest inhibition zone of 30 µL Au NPs was 12 mm for *Streptococcus pyogenes*. The gold nanoparticles revealed high inhibitory effect to frustrate the growth of these micro-organisms when compared to the antibiotic chloramphenicol. Chwalibog et al. inferred that the size of Au NPs was 250 times smaller than that

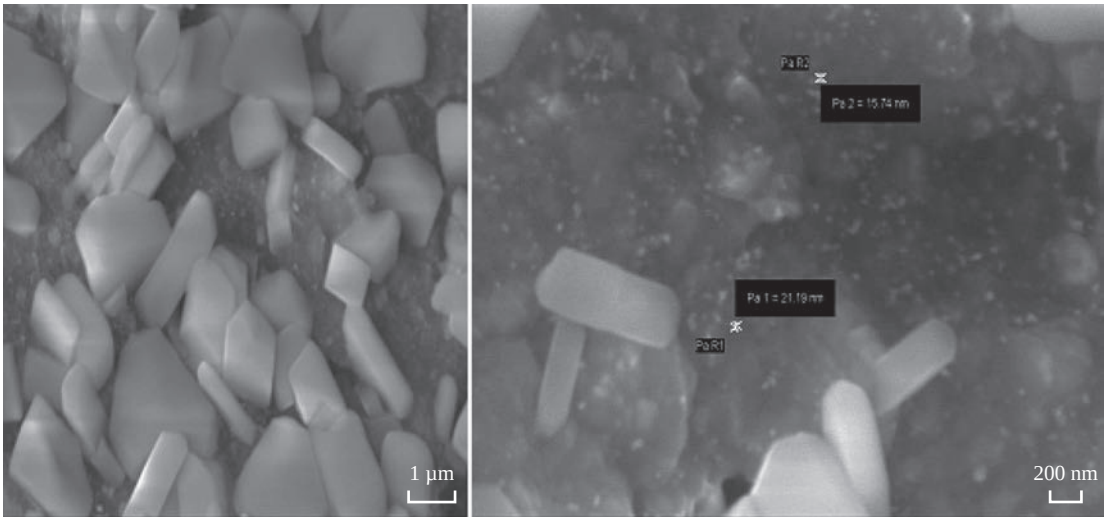

Fig. 5 Scanning electron microscope images of gold nanoparticles using *C. cretica* leaf extract at different magnifications.

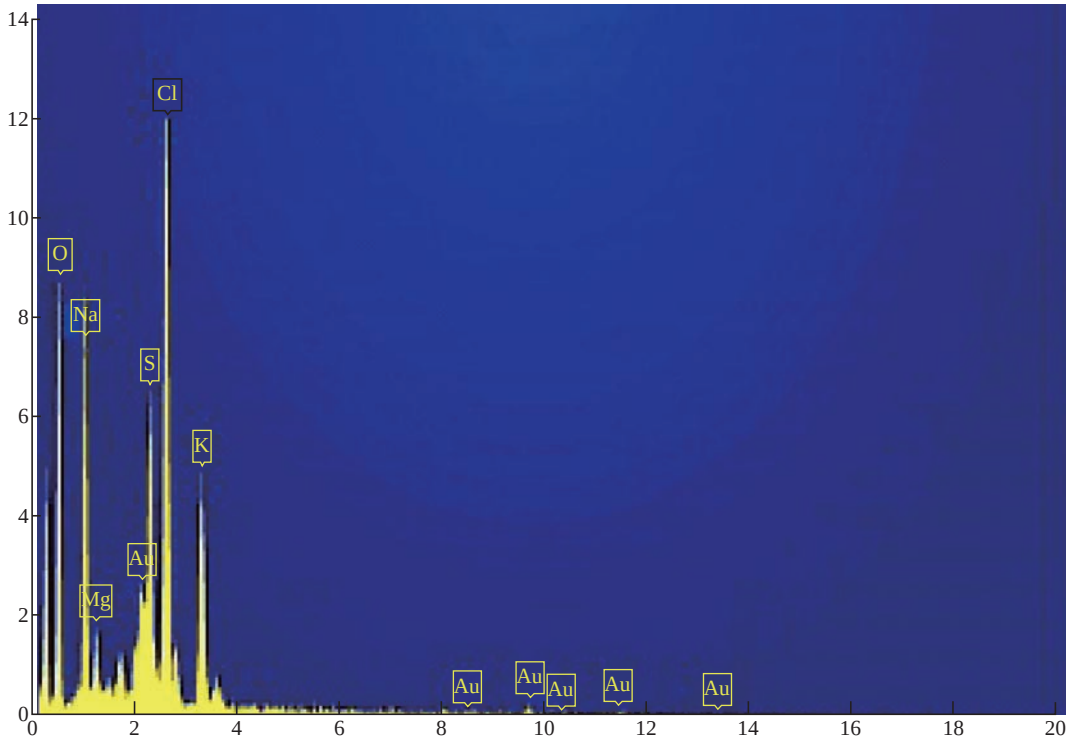

Fig. 6 Energy dispersive X-ray spectroscopyimage of gold nanoparticles using *C. cretica* leaf extract.

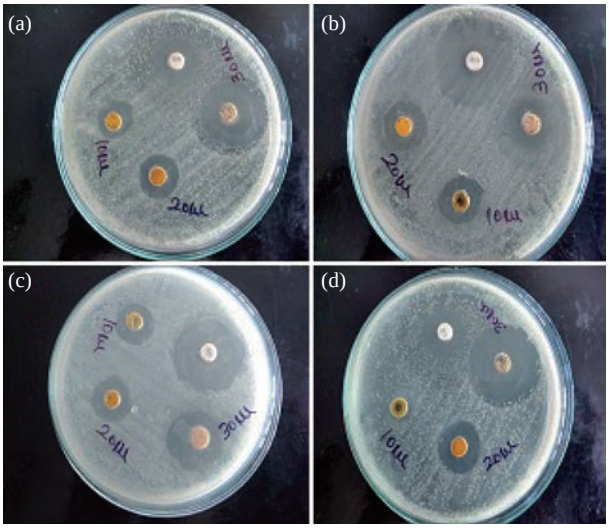

Fig. 7 Antibacterial efficacy of Au NPs against human pathogenic bacteria: **(a)** *Escherichia coli*; **(b)** *Klebsiella pneumonia*; **(c)** *Staphylococcus aureus*; and **(d)** *Streptococcus pyogenes*.

of a bacterium and the Au NPs could easily adhere to the microorganisms' cell surface inducing its deformation, which might cause the death of microorganism [45]. Recently, various research reports focused on the exact mechanism of antibacterial activity of Au NPs, however it is not still known. Wani et al. studied that the influence of sizes of Au NPs on their inhibitory effect against micro-organism and suggested that gold ions released from the Au NPs might interact with sulphur and phosphorus-containing biomolecules like protein and DNA and led to degrading their structures and disrupting the metabolic processes [37]. Small-sized gold nanoparticles have greater toxicity. In our present study (Table1), the gram-negative bacteria revealed higher inhibition zone than gram-positive bacteria. The small-sized gold nanoparticles could easily pierce the cell membrane of gram-negative

Table 1 Zone of inhibition (mm) of Au NPs using *Cressa cretica* leaf extract against human pathogenic bacteria

S. No	Pathogenic bacteria	Zone of inhibition in diameter (mm)			
		Concentration (µg/mL)			Chloramphenicol (10 µg) (control)
		10 µL	20 µL	30 µL	
1.	*Streptococcus pyogenes*	3	7	12	6
2.	*Staphylococcus aureus*	5	6	8	8
3.	*Escherichia coli*	5	7	10	5
4.	*Klebsiella pneumoniae*	5	7	7	10

bacteria compared to the cell membrane of gram-positive bacteria owing to that the cell membrane of gram-negative bacteria was made of a thin layer of peptidoglycan compared to the cell membrane of gram-positive bacteria [46]. Recently, several reports have suggested that Au NPs have been found to generate reactive oxygen species (ROS), which may lead to the death of bacteria's cells [22]. The antibacterial activity studies exhibited that the gold nanoparticles using *Cressa cretica* leaf extract showed notable antibacterial activity against human pathogens. Earlier, Sunita et al. suggested that *Cressa cretica* plant extract had a significant inhibitory effect against human pathogenic bacterial strains [30]. FTIR and EDX studies of the Au NPs using *C. cretica* leaf extract revealed that some of the biological moieties of *C. cretica* leaf extract adhered on the surface of the biofabricated Au NPs. The biological moieties of the *C. cretica* leaf extract also enhanced the antibacterial efficacy of the Au NPs against human pathogenic bacterial strains.

Catalytic reduction of 4-nitrophenol

The catalytic efficacy of biofabricated gold nanoparticles was evaluated by the reduction of 4-nitrophenol using sodium borohydride in alkaline medium [27]. The catalytic efficacy of the biofabricated gold nanoparticles was scanned using UV-Vis spectroscopy in the range of 250-600 nm at particular time intervals. 4-nitrophenol exhibited an absorbance peak at ~314 nm. The absorption peak was shifted to 400 nm after the adding of the $NaBH_4$ solution, indicating the formation of the 4-nitrophenolate ion. The absorption peak remained constant at 400 nm in the absence of Au NPs for long duration. It showed that $NaBH_4$ itself did not have the potential to reduce the 4-nitrophenol. 4-nitrophenol was converted to 4-aminophenol, resulting in reduced absorption peak in 400 nm and increased absorption peak in 296 nm in the presence of Au NPs (Fig. 8), indicating the formation of 4-aminophenol [25, 28].

The reduction reaction was completed within 54 min as was evident from the disappearance of yellow colour. Here the Au NPs acted as an electron transfer mediator between 4-nitrophenol and $NaBH_4$. The catalytic reduction proceeded on the surface of the Au NPs. As soon as the electron acceptor (4-nitrophenol) and the electron donor (borohydride ion) were adsorbed on surface of the biofabricated Au NPs, the catalytic reduction reaction began via the transfer of electrons from borohydride ions to 4-nitrophenol.

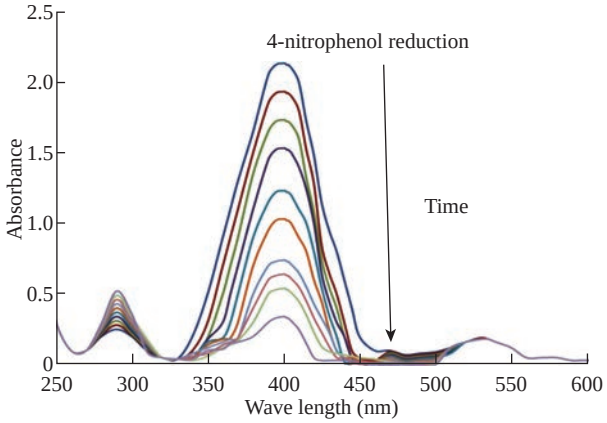

Fig. 8 Ultraviolet-visible absorption spectra for the catalytic reduction of 4-nitrophenol by $NaBH_4$ in the presence of AuNPs using *C. cretica* leaf extract.

Thus, Au NPs helped in assisting the reduction of 4-nitrophenol by lowering the activation energy of the reaction. Hence, the Au NPs acted as a catalyst [47]. Since the concentration of $NaBH_4$was much higher than 4-nitrophenol, the rate of reduction could be considered independent of $NaBH_4$ concentration and dependent of 4-nitrophenol concentration. The catalytic rate constant (k) was evaluated using the pseudo-first-order kinetics equation:

$$\ln (A_t / A_0) = -kt,$$

where A_0 is an initial absorbance of the reaction, A_t is absorbance in time t, and k is rate constant of the reaction. The rate constant (k) for the reduction of 4-nitrophenol was found to be 0.033 min^{-1} (Fig. 9). Thus, the biofabricated Au NPs acted as a predominant catalyst for the reduction reactions of toxic chemicals like 4-nitrophenol and could be successfully used for wastewater treatment.

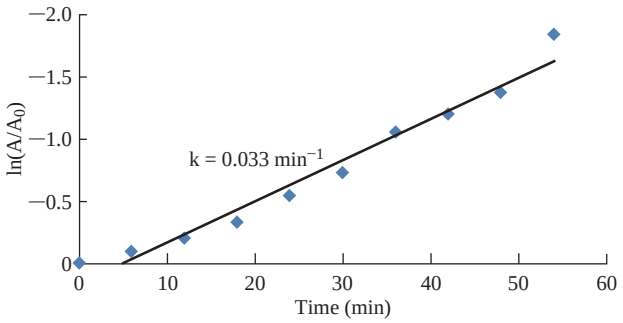

Fig. 9 Kinetic curve of 4-nitrophenol reduction catalyzed by Au NPs using *C. cretica* leaf extract.

Conclusions

In the present investigation, the single step, cost-effective and green protocols were developed to

synthesize the biofabricated gold nanoparticles using *Cressa cretica* leaf extract. The UV-Vis spectrum displayed a peak at 539 nm which confirmed the formation of biofabricated Au NPs. The gold nanoparticles were highly crystalline in nature with the particle size of 15-22 nm as detected and confirmed by XRD. The FTIR studies suggested that the hydroxyl, amide and amine groups of *Cressa cretica* leaf extract were responsible for the formation and stabilization of the Au NPs. The SEM studies revealed that the biofabricated AuNPs were of hexagonal, pentagonal, spherical and rod shapes with 15-22 nm in size. The biofabricated Au NPs showed significant antimicrobial efficacy against human pathogens. The biofabricated AuNPs were also found to be a highly efficient catalyst in organic transformation for bioremediation. Thus, the Au NPs are anticipated to be a strong candidate for biomedical applications and environmental bioremediation.

Acknowledgements

Authors gratefully acknowledge the International Research Centre, Kalasalingam University, Krishnankoil, India for providing FTIR, XRD and SEM facilities, STIC, Kochi, India for providing EDX facility, and Bharathiar University, Coimbatore, India for providing antibacterial experimentation.

Conflict of Interests

The authors declare that no competing interest exists

References

[1] J.L. Gardea-Torresdey, J.G. Parsons, E. Gomez, et al., Formation and growth of au nanoparticles inside live Alfalfa Plants. *Nano Letter*, 2002, 2: 397-401.

[2] J.E. Hutchison, Greener nanoscience: a proactive approach to advancing applications and reducing implications of nanotechnology. *ACS Nano*, 2008, 2: 395-402.

[3] S. Soman, J. Ray, Phytosynthesis and characterization of silver nanoparticles using leaf extracts of Premna serratiffolia L. *Nano Biomed Eng*, 2013, 5: 148-152.

[4] N.A. Begum, S. Mondal, S. Basu, et al., Biogenic synthesis of Au and Ag nanoparticles using aqueous solutions of black tea leaf extracts. *Colloids Surf B Biointerfaces*, 2009, 71: 113-118.

[5] X. Huang, P.K. Jain, I.H. EI-Sayed, et al., Gold nanoparticles: interesting optical properties and recent applications in cancer diagnostic and therapy. *Nanomedicine*, 2007, 2: 681-693.

[6] A.K. Jha, K. Prasad, and A.R. Kulkarni, Synthesis of TiO_2 nanoparticles using microorganism. *Colloids Surf B Biointerfaces*, 2009, 71: 226-229.

[7] I. Willner, R. Baron, and B. Willner, Growing metal nanoparticles by enzymes. *Adv Mater*, 2006, 18: 1109-1120.

[8] M. Jain, R. Kapadia, R.N. Jadeja, et al., Traditional uses, phytochemistry and pharmacology of Tecomella undulate - a review. *Asian Pacific Journal of Tropical Biomedicine*, 2012, 2: S1918-S1923.

[9] A.K. Mittal, Y. Chisti, and U.C. Banerjee, Synthesis of metallic nanoparticles using plant extract. *Biotechnol Adv*, 2013, 13: 346-356.

[10] V. Kumar, S.K. Yadav, Plant-mediated synthesis of silver and gold nanoparticles and their applications. *J Chem Techonl Biotechnol*, 2009, 84: 151-157.

[11] S. Narayanan, B.N. Sathy, U. Mony, et al., Biocompatible magnetite/gold nanohybrid contrast agents via green chemistry for MRI and CT bioimaging. *ACS Appl Mater Interfaces*, 2012, 4: 251-260.

[12] H.S. Sharma, S.F. Ali, S.M. Hussain, et al., Influence of engineered nanoparticles from metals on the blood-brain barrier permeability, cerebral blood flow, brain edema and neurotoxicity. An experimental study in the rat and mice using biochemical and morphological approaches. *J Nanosci Nanotechnol*, 2009, 9: 5055-5072.

[13] P. Raveendran, J. Fu, and S.L. Wallen, Completely "green" synthesis and stabilization of metal nanoparticles. *J Am Chem Soc*, 2003, 125: 13940-13941.

[14] S. Balasubramanian, U. Jeyapaul, and S. Mary Jelastin Kala, Ecofriendly synthesis of silver nanoparticles using ethno medicinal plant leaf extract (Jasminum Auriculatum) and their antibacterial properties. *International Letters of Chemistry, Physics and Astronomy*, 2015, 58: 113-121.

[15] D.S. Sheny, J. Mathew, and D. Philip, Phytosynthesis of Au, Ag and Au-Ag bimetallic nanoparticles using aqueous extract and dried leaf of Anacardium occidentale. *Spectrochim Acta A Mol Biomol Spectrosc*, 2011, 79: 254-262.

[16] S. Balasubramanian, U. Jeyapaul, A. John Bosco, et al., Green synthesis of silver nanoparticles using Cressa Cretica leaf extract and its antibacterial efficacy. *International Journal of Advanced Chemical Science and Applications*, 2015, 3: 65-71.

[17] D. Baruah, M. Goswami, R.N.S. Yadav, et al., Biogenic synthesis of gold nanoparticles and their application in photocatalytic degradation of toxic dyes. *Journal of Photochemistry and Photobiology B: Biology*, 2018, 186: 51-58.

[18] A. Das, G. Shanker, C. Nath, et al., A comparative study in rodents of standardized extracts of Bacopa monniera and Ginkgo biloba: anticholinesterase and cognitive enhancing activities. *Pharmacol Biochem Behav*, 2002, 73: 893-900.

[19] N. Kulkarni, U. Muddapur, Biosynthesis of metal nanoparticles: A review. *J Nanotechnol*, 2014, 2014: 510246.

[20] A.K. Jha, K. Prasad, K. Prasad, et al., Plant system: Nature's nanofactory. *Colloids Surf B Biointerfaces*, 2009, 73: 219-223.

[21] B. Casciaro, F. Cappiello, M. Cacciafesta, et al., Promising approaches to optimize the biological properties of the antimicrobial peptide esculentin-1a(1-21)NH_2: Amino acids substitution and conjugation to nanoparticles. *Front Chem*, 2017, 5: 26.

[22] S. Senthilkumar, L. Kashinath, M. Ashok, et al., Antibacterial properties and mechanism of gold nanoparticles obtained from Pergularia daemia leaf. *J Nanomed Res*, 2017, 6: 00146.

[23] V.P. Zharov, K.E. Mercer, E.N. Galitovskaya, et al., Photothermal nanotherapeutics and nanodiagnostics for selective killing of bacteria targeted with gold

nanoparticles. *Biophys J*, 2006, 90: 619-627.
[24] X. Huang, I.H. El-Sayed, W. Qian, et al., Cancer cell Imaging and Photothermal therapy in the Near-Infrared Region by using gold nanorods. *J Am Chem Soc*, 2006, 128: 2115-2120.
[25] M. Kumari, A. Mishra, S. Pandey, et al., Physico-chemical condition optimization during biosynthesis lead to development of improved and catalytically efficient gold nanoparticles. *Scientific Reports*, 2016, 6: 27575.
[26] S. Joseph, B. Mathew, Microwave-assisted facile green synthesis of silver and gold nanocatalysts using the leaf extract of Aerva lanata. *Spectrochim Acta A Mol Biomol Spectrosc*, 2015, 136: 1371-1379.
[27] M.F. Zayed, W.H. Eisa, Pheonix dactylifera L. leaf extract phytosynthesized gold nanoparticles; controlled synthesis and catalytic activity. *Spectrochim Acta A Mol Biomol Spectrosc*, 2014, 121: 238-244.
[28] A. Rajan, M. MeenaKumari, and D. Philip, Shape tailored green synthesis and catalytic properties of gold nanocrystals. *Spectrochim Acta A Mol Biomol Spectrosc*, 2014, 118: 793-799.
[29] S. Priyashree, S. Jha, and S.P. Pattanayak, A review on Cressa cretica Linn: A halophytic plant. *Pharmacogn Rev*, 2010, 4: 161-166.
[30] P. Sunita, S. Jha, S.P. Pattanayak, et al., Antimicrobial activity of a halophytic plant Cressa cretica L. *J Sci Res*, 2012, 4: 203-212.
[31] Anonymous, *Pharmacopoeia of India* (third edition). Ministry of health and family welfare, Government of India, 1996.
[32] M. Sheikh, A.R. Malik, M.K. Meghavanshi, et al., Studies on some plant extracts for their antimicrobial potential against certain pathogenic microorganisms. *American Journal of Plant Sciences*, 2012, 3: 209-213.
[33] A. Gangula, R. Podila, M. Ramakrishna, et al., Catalytic reduction of 4-nitrophenol using biogenic gold and silver nanoparticles derived from Breynia rhamnoides. *Langmuir*, 2011, 27: 15268-15274.
[34] S.K. Chaudhuri, S. Chandela, and L. Malodia, Plant mediated green synthesis of silver nanoparticles using Tecomella undulata leaf extract and their characterization. *Nano Biomed Eng*, 2016, 8: 1-8.
[35] P. Rajasekharreddy, P.U. Rani, and B. Sreedhar, Qualitative assessment of silver and gold nanoparticle synthesis in various plants: a photobiological approach. *J Nanopart Res*, 2010, 12: 1711-1721.
[36] E. Pretsch, P. Bühlmann, and M. Badertscher, Structure determination of organic compounds. *Springer-Verlag Berlin Heidelberg*, 2009: 49-68.
[37] I.A. Wani, T. Ahmad, Size and shape dependant antifungal activity of gold nanoparticles: A case study of Candida. *Colloids Surf B Biointerfaces*, 2013, 101: 162-170.
[38] B.S. Bhau, S. Ghosh, S. Puri, et al., Green synthesis of gold nanoparticles from the leaf extract of Nepenthes khasiana and antimicrobial assay. *Adv Mater Lett*, 2015, 6: 55-58.
[39] A. Sett, M. Gadewar, P. Sharma, et al., Green synthesis of gold nanoparticles using aqueous extract of Dillenia indica. *Adv Nat Sci Nanosci Nanotechnol*, 2016, 7: 025005.
[40] J.Y. Song, B.S. Kim, Rapid biological synthesis of silver nanoparticles using plant leaf extracts. *Bioprocess Biosyst Eng*, 2008, 32: 79-84.
[41] S.H. Lim, E.Y. Ahn, and Y. Park, Green synthesis and catalytic activity of gold nanoparticles synthesized by Artemisia capillaris water extract. *Nanoscale Res Lett*, 2016, 11: 474.
[42] V. Ramesh, A. Armash, Green synthesis of gold nanoparticles against pathogens and cancer cells. *International Journal of Pharmacological Research*, 2015, 5: 250-256.
[43] C. Wang, R. Mathiyalagan, Y.J. Kim, et al., Rapid green synthesis of silver and gold nanoparticles using Dendropanax morbifera leaf extract and their anticancer activities. *Int J Nanomedicine*, 2016, 11: 3691-3701.
[44] S. Balasubramanian, U. Jeyapaul, and S. Mary Jelastin Kala, Antibacterial activity of silver nanoparticles using Jasminum auriculatum stem extract. *International Journal of Nanoscience*, 2018, 17(3): 1850011.
[45] A. Chwalibog, E. Sawosz, A. Hotowy, et al., Visualization of interaction between inorganic nanoparticles and bacteria or fungi. *Int J Nanomedicine*, 2010, 5: 1085-1094.
[46] Y. Zhou, Y. Kong, S. Kundu, et al., Antibacterial activities of gold and silver nanoparticles against Escherichia coli and bacillus Calmette-Guérin. *J Nanobiotechnology*, 2012, 10: 19.
[47] S.A. Aromal, D. Philip, Green synthesis of gold nanoparticles using Trigonella foenum-graecum and its size-dependent catalytic activity. *Spectrochim Acta A Mol Biomol Spectrosc*, 2012, 97: 1-5.